Available online at www.sciencedirect.com

ScienceDirect

IFAC Papers Online CONFERENCE PAPER ARCHIVE

IFAC-PapersOnLine 49-10 (2016) 059–064

Passive suppression of thermoacoustic instability in a Rijke tube

Umut Zalluhoglu*, Nejat Olgac**

**University of Connecticut, Storrs, CT 06269-3139 USA (e-mail: umut.zalluhoglu@uconn.edu).*
*** University of Connecticut, Storrs, CT 06269-3139 USA (e-mail: olgac@engr.uconn.edu)*

Abstract: This article investigates passive stabilization of thermoacoustic dynamics in a Rijke tube by using a Helmholtz resonator. Under certain assumptions, the mathematical model of the dynamics is shown to fall into the linear time-invariant multiple time delay systems class of neutral type. To study the thermoacoustic instability phenomenon and its passive suppression, the cluster treatment of characteristic roots (CTCR) paradigm is implemented. This effort reveals the placement of Helmholtz resonator along the Rijke tube for stabilizing the unstable dynamics. The analytically obtained results are compared with experiments conducted on a laboratory scale Rijke tube. In addition, the effect of resonator's design parameters on its stabilization capability is investigated.

1. INTRODUCTION

Thermoacoustic instability (TAI) is a major problem for gas turbines since it results in undesired vibrations in the combustor and raises fatigue concerns. TAI primarily results from the interaction of heat release and acoustic disturbances. The regionally confined unsteady heat release drives the acoustic waves in the combustion chamber. They propagate along the combustor, reflect from the boundaries, return and meet with the heat source again with some time delays. This causes disturbances in heat release rate, which amplifies the oscillations when synchronized (Rayleigh, 1878).

Many researchers focus on simpler thermoacoustic devices such as a Rijke tube, to have a better understanding of the problem (Dowling and Morgans, 2005; Gelbert et al., 2012; Olgac et al., 2014; Zalluhoglu et al., 2016). Similarly, we use the Rijke tube as the platform to study and control TAI phenomenon in this paper. TAI control attempts can be divided into two classes: active and passive methods. The former is usually achieved by forming a feedback loop that modulates the acoustic pressure or fuel injection rates to eliminate TAI (Dowling and Morgans, 2005; Banaszuk et al., 2004; Olgac et al., 2015; Zalluhoglu and Olgac, 2015). In practice; however, active control has some drawbacks such as requirement of high actuation power, limited bandwidth, and potential to invite more instability, which make passive approach more favourable. Among many passive approaches such as altering the chamber design, installing resonators, baffles and acoustic liners to the combustor, we focus on the utilization of a Helmholtz resonator to attenuate TAI.

Helmholtz resonator is a simple encapsulated air cavity as shown in Fig. 1. Once mounted on a duct, it imparts noise reduction within a frequency band. A single degree of freedom (SDOF) model of the resonator is derived in (Kinsler et al., 1996; Kim and Selamet, 2011) akin to a mechanical vibration absorber (see Fig. 1). The mass of air at the neck of the resonator oscillates against the volume of air in the cavity when excited by external pressure. The air in the larger cavity exerts a counter force resembling the spring and damper forces in mechanical vibration absorbers. Helmholtz resonators are used as acoustic dampers to abate the combustion-excited oscillations (Zhao and Morgans, 2009).

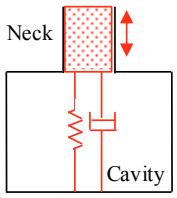

Fig. 1. Helmholtz resonator (black) and its analogy to a mechanical vibration absorber (red).

A critical issue in this application is the placement of the resonator. As observed in Cora et al., (2014), wrong placements may result in amplification of pressure oscillations. The main contribution of this paper is in the development of an analytical guideline to resolve this issue. We first develop a linear time-invariant neutral multiple time delay system (LTI-NMTDS) model that represents the dynamics in the Helmholtz resonator mounted Rijke tube. Then we analytically determine the stabilizing resonator locations along the tube for an initially unstable operation and compare it with experimental results. In addition, the effect of resonator's design parameters on its stabilization capability investigated.

In order to assess stability of LTI-NMTDS, numerical algorithms that approximate the characteristic root locations (Vyhlidal and Zitek, 2009) and methods utilizing Lyapunov-Krasovskii theory (Gu and Niculescu, 2006) are widely used. Nevertheless, the former approach becomes computationally demanding over large range of delays and the latter method provides conservative results for stability. Alternatively, the Cluster Treatment of Characteristic Roots (CTCR) paradigm (Olgac et al., 2005) analytically declares the necessary and sufficient conditions for stability of such systems. The strength of this paradigm is that it can assess the stability over very broad range of time delays exhaustively and non-conservatively. It is used as the facilitating stability analysis tool throughout the paper.

10.1016/j.ifacol.2016.07.473

2. THE MATHEMATICAL MODEL

The model described here carries the dynamics of the Rijke tube mounted with a Helmholtz resonator under commonly applied assumptions (Dowling and Morgans, 2005, Olgac et al., 2014): (i) the airflow is induced by natural buoyancy, therefore has negligibly small Mach number; (ii) the average (mean) flow quantities such as density $\bar{\rho}$ and the speed of sound $\bar{c}$ are assumed as constant along the tube; (iii) the acoustic wave propagation is taken as 1-D event.

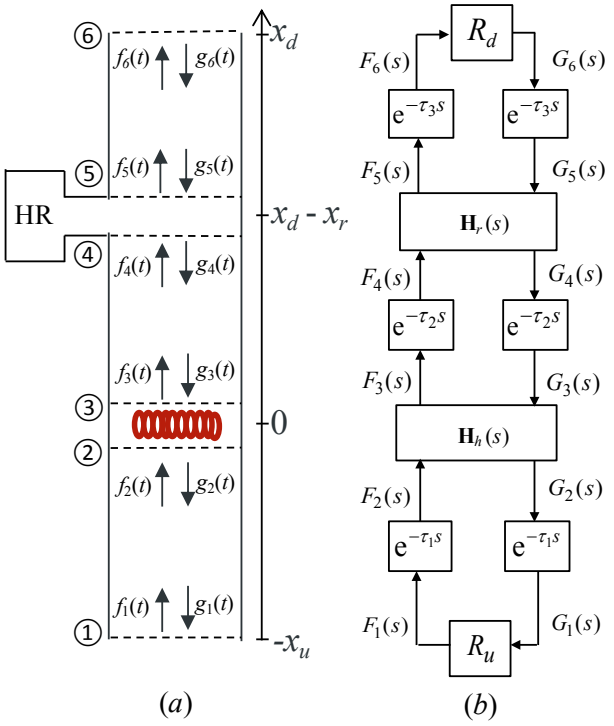

Fig. 2. (a) Schematic representation of Helmholtz resonator mounted Rijke tube dynamics, (b) its block diagram

The thermoacoustic dynamics is governed by the first principles, conservation of mass, momentum and energy, which are partial differential equations. When linearized under the listed assumptions, the pressure and velocity fluctuations within the tube obey the linear wave equation. Using the d'Alembert solution, they are expressed as

$$\tilde{p}(x,t) = f(t - x/\bar{c}) + g(t + x/\bar{c}) \quad (1)$$

$$\tilde{u}(x,t) = [f(t - x/\bar{c}) - g(t + x/\bar{c})]/\bar{\rho}\bar{c} \quad (2)$$

where overscript $\tilde{\bullet}$ denotes the non-steady (i.e., fluctuating) and $\bar{\bullet}$ represents the steady (mean) components of the quantity $\bullet$. $f(x,t)$ and $g(x,t)$ represent the acoustic waves traveling upwards and downwards in the tube, respectively. As shown in Fig. 2a, x is the position along the tube, where $x = 0$ corresponds to location of the heater. At the tube ends $x = -x_u$ and $x = x_d$, where x_u and x_d denote the distances between ①-② and ③-⑥ (the upstream and downstream sides from the heating zone), respectively. The resonator is mounted at $x = x_d - x_r$ (i.e. x_r below the downstream end).

The block diagram of the overall dynamics is given in Fig. 2b. In this representation, the system variables are the acoustic waves $f_i(t)$ and $g_i(t)$. The subscript $i = 1,\ldots,6$ denotes the cross-sections in Fig. 2a, where these functions are evaluated. The time delays $\tau_1 = x_u/\bar{c}$, $\tau_2 = (x_d - x_r)/\bar{c}$ and $\tau_3 = x_r/\bar{c}$ correspond to the travel times of acoustic waves moving at the speed of sound. Utilizing the causal relationships between each variable in Fig. 2b, one can write

$$\begin{pmatrix} F_1(s) \\ G_4(s) \\ F_3(s) \\ G_6(s) \end{pmatrix} = \mathbf{R} \begin{pmatrix} G_1(s) \\ F_3(s) \\ G_4(s) \\ F_6(s) \end{pmatrix}, \quad \mathbf{R} = \begin{bmatrix} R_u & 0 & 0 & 0 \\ 0 & 0 & 1 & 0 \\ 0 & 1 & 0 & 0 \\ 0 & 0 & 0 & R_d \end{bmatrix} \quad (3)$$

in Laplace domain. Here, R_u and R_d are the reflection coefficients that characterize the boundary conditions at cross-sections ① and ⑥. The input vector in (3) can be expressed as

$$\begin{pmatrix} G_1(s) \\ F_3(s) \\ G_4(s) \\ F_6(s) \end{pmatrix} = \mathbf{T}_1 \begin{pmatrix} G_2(s) \\ F_3(s) \\ G_4(s) \\ F_5(s) \end{pmatrix}, \quad \mathbf{T}_1 = \begin{bmatrix} e^{-\tau_1 s} & 0 & 0 & 0 \\ 0 & 1 & 0 & 0 \\ 0 & 0 & 1 & 0 \\ 0 & 0 & 0 & e^{-\tau_3 s} \end{bmatrix} \quad (4)$$

Next, using the transfer matrices $\mathbf{H}_h$ and $\mathbf{H}_r$ that represent the interaction of acoustic waves at the heating zone $(x = 0)$ and resonator zone $(x = x_d - x_r)$, respectively, one obtains

$$\begin{pmatrix} G_2(s) \\ F_3(s) \\ G_4(s) \\ F_5(s) \end{pmatrix} = \mathbf{H} \begin{pmatrix} F_2(s) \\ G_3(s) \\ F_4(s) \\ G_5(s) \end{pmatrix}, \quad \mathbf{H} = \begin{bmatrix} \mathbf{H}_h & \mathbf{0}_2 \\ \mathbf{0}_2 & \mathbf{H}_r \end{bmatrix} \quad (5)$$

Here, $\mathbf{0}_2$ represents a zero matrix of size 2×2. More information on $\mathbf{H}_h$ and $\mathbf{H}_r$ matrices can be found in Appendices A and B, respectively. Similar to (4), the input vector in (5) can be expressed as

$$\begin{pmatrix} F_2(s) \\ G_3(s) \\ F_4(s) \\ G_5(s) \end{pmatrix} = \mathbf{T}_2 \begin{pmatrix} F_1(s) \\ G_4(s) \\ F_3(s) \\ G_6(s) \end{pmatrix} \mathbf{T}_2 = \begin{bmatrix} e^{-\tau_1 s} & 0 & 0 & 0 \\ 0 & e^{-\tau_2 s} & 0 & 0 \\ 0 & 0 & e^{-\tau_2 s} & 0 \\ 0 & 0 & 0 & e^{-\tau_3 s} \end{bmatrix} \quad (6)$$

Combining the transfer matrices (3), (4), (5) and (6) to close the loop in Fig. 2b, one gets

$$\begin{pmatrix} F_1(s) \\ G_4(s) \\ F_3(s) \\ G_6(s) \end{pmatrix} = \mathbf{R}\mathbf{T}_1\mathbf{H}\mathbf{T}_2 \begin{pmatrix} F_1(s) \\ G_4(s) \\ F_3(s) \\ G_6(s) \end{pmatrix} \quad (7)$$

which yields